

A PARAMETRIC STUDY OF FRICTION RIVETING ON THE DISIMILAR JOINT FORMATION AND STRENGTH

Damjan Klobčar¹, Haidi Škrabar¹, Franci Pušavec¹, Drago Bračun¹,
Aljaž Ščetinec¹, Ivan Jurič², Ivica Garašič², Zoran Kožuh²,

¹Faculty of Mechanical Engineering, University of Ljubljana, Slovenia, *correspondence: damjan.klobcar@fs.uni-lj.si
²Faculty of Mechanical Engineering and Naval Architecture, University of Zagreb, Croatia

ABSTRACT

Similar or dissimilar materials in aerospace applications can be joined using friction. In this way a certain CRM components of titanium alloys, stainless steel and magnesium alloys can be replaced by aluminium alloys or composites. Such replacement can reduce the weight of aerospace component and substantially reduce the fuel consumption and CO₂ emissions. The present work shows the effect of friction riveting parameters on the anchoring effect and joint strength. The materials used are aluminium alloy 2024 and polyetherimide. After the riveting the joints were examined by X-ray, which showed an insight into the joint geometry and anchoring shape of the rivet. Part of the joints were tested with pull-out test and from the rest macro-sections were prepared. Samples produced with higher mechanical energy achieved greater anchoring depths of rivets into the polymeric base plates and consequently higher pull-out forces. It was established that the most important parameters are friction force and time of the first phase of friction riveting process. Higher energy input in the first phase is reflected in higher rivet deformation i.e. higher anchoring effect.

Keywords: friction riveting, reduction of CRM's, aluminium alloy 2024, polyetherimide, pull-out test, NDT

MATERIALS AND METHODS

The subject of the study were rivets made of aluminum rods (Fig. 1) grade 2024-T351 in the polyetherimide (PEI) base material (24x24x14 mm). Rivets were made with a CNC Doosan NX 6500 II Aluminum rods (Fig. 1) were clamped in the machine at the thinner section. Additionally, Fig. 1 shows friction riveting process.

Rivet formation was section in two phases where each of the phases had different combination of the feed speed V_f , and penetration depth Z .

1. Aluminum rod made contact with the base material and heating due friction initiated followed by the insertion of the rod in the base material
2. Increase of feed speed and insertion depth followed by stopped rotation and consolidation.

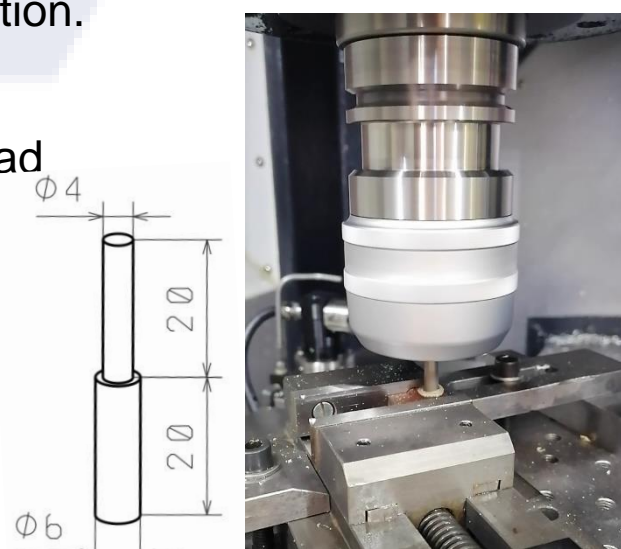


Figure 1: Aluminum rivet dimension and riveting process

Process parameters

Spindle speed was a constant at 20000 min⁻¹. Z in the first phase was 5 mm, 9 mm and 10 mm while V_f was either 100 mm/min or 200 mm/min. In the second phase Z was 10 mm, 15 mm, 19 mm or 20 mm. While V_f was 900 mm/min, 1200 mm/min, 1800 mm/min or 2000 m/min. Parameters for each rivet are shown in the table 1.

Sample nr.	Phase 1		Phase 2	
	Z [mm]	V _f [mm/min]	Z [mm]	V _f [mm/min]
1	5	100	10	1200
2	5	200	15	2000
3	10	200	20	1200
4	10	200	20	1800
5	10	200	20	900
6	9	200	20	900
7	9	200	19	900

Destructive and non-destructive testing

To determine the quality of friction rivets, they were examined by means of X-ray tomography and pull-out test. X-ray tomography showed an insight into the joint geometry and anchoring shape of the rivet. Part of the joints were tested with a pull-out test. From the remainder macro-sections were prepared.

Modelling of the process

Heat input (E_M) was modelled by calculation of mechanical energy, as shown in the Equation 1

$$E_M = E_{T1} + E_{T2} = \int T1 \times \omega \times dt + \int T2 \times \omega \times dt [J] \quad \text{Eq. 1}$$

Where E_{T1} And E_{T2} represent energy input through torque (T) and angular velocity (ω) in the first and second phase of river formation.

The volumetric ratio [0-1] (Eq. 2) establishes a simplified quotient between the volume of the plastically deformed rivet and the volume of polymer offering mechanical resistance to a rivet pull-out action. The volumetric ratio (VR) is determined by Equation 2. Equation components are explained with the assist of the Fig. 2. H is the penetration depth, B the deformed tip height, W the maximum deformed width of the rivet tip and D the original rivet diameter

$$VR = \frac{(W^2 - D^2) \cdot D_p}{H \cdot W^2} [J] \quad \text{Eq. 2}$$

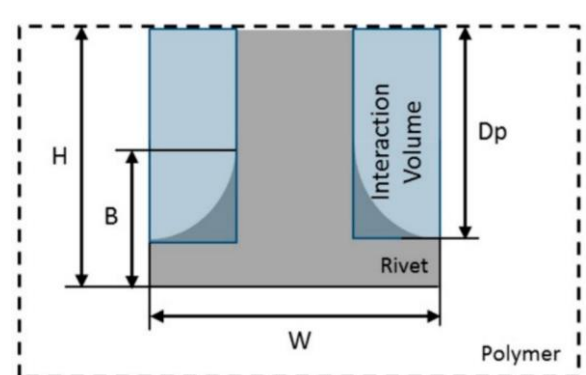


Figure 2: Volumetric ratio and interaction volume in a friction rivet

RESULTS

X-ray tomography

Dimensions of all rivets are shown in the Fig 3, along with the corresponding volumetric ratio. Example of rivet dimensions measurement is shown in Fig 4.

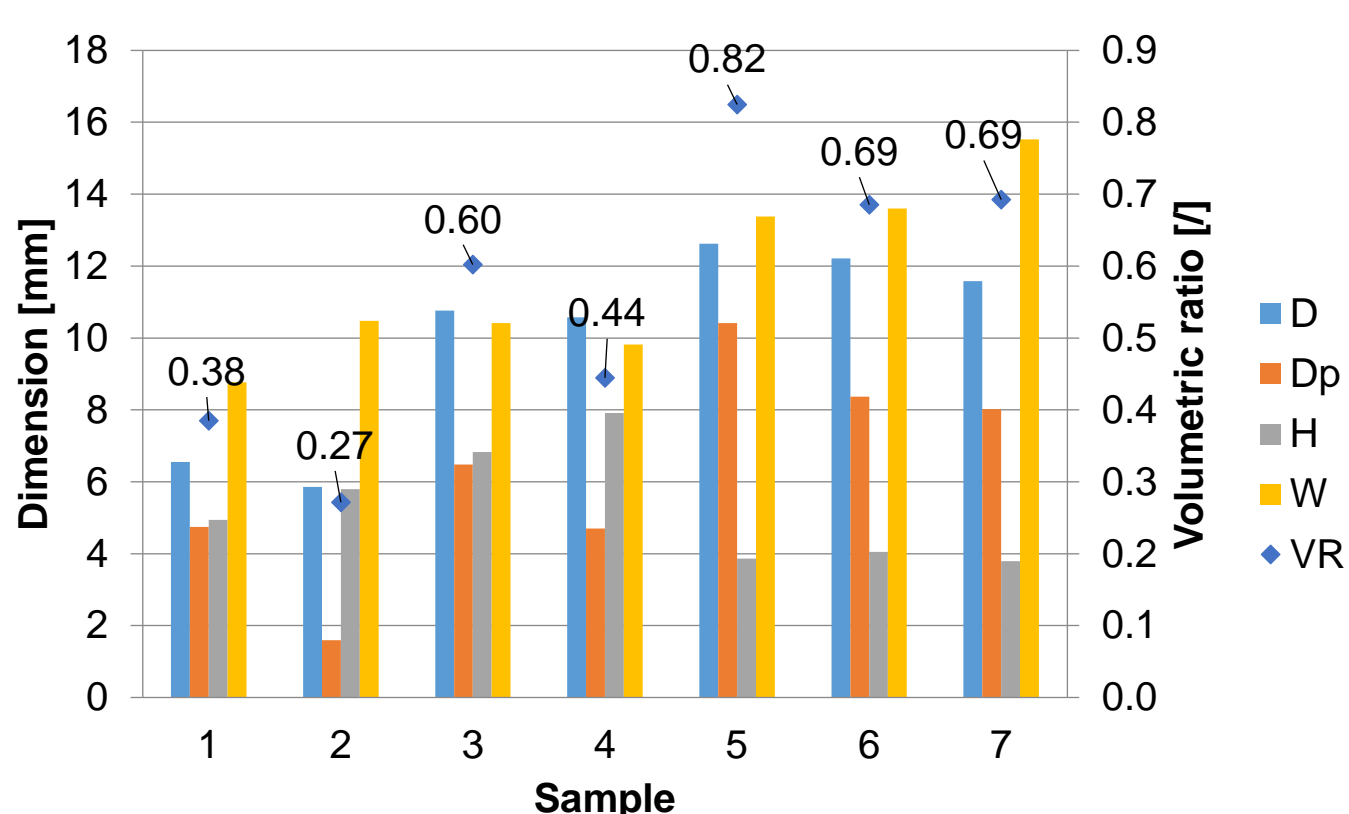


Figure 3: Friction rivet dimensions and corresponding volumetric ratios

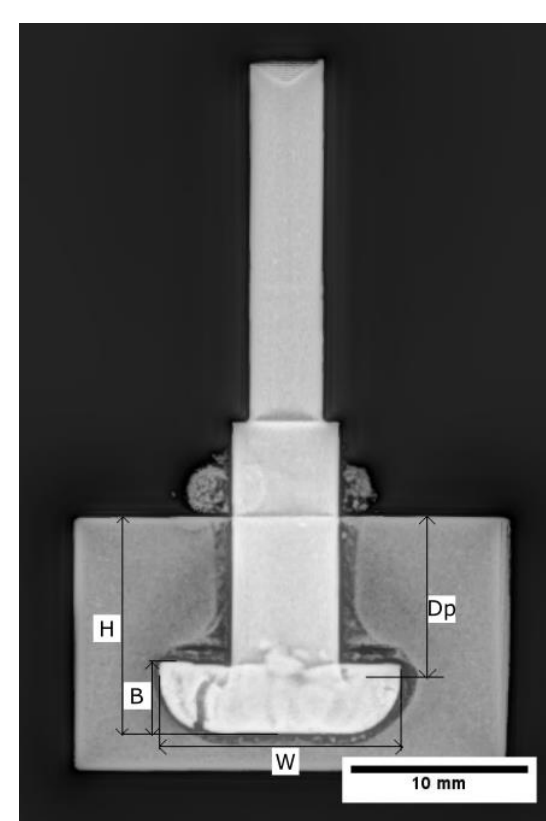


Figure 3: Friction rivet dimensions measurement.

X-ray Tomography

Figure 5 shows X-ray tomography images of all rivets. In addition to dimensions measurements, each image was examined for possible defects in the joint. Three different joint shapes were recognized: anchor (5, 6, 7), bell with decreasing diameter (3), bell with highest diameter at the end of rivet.

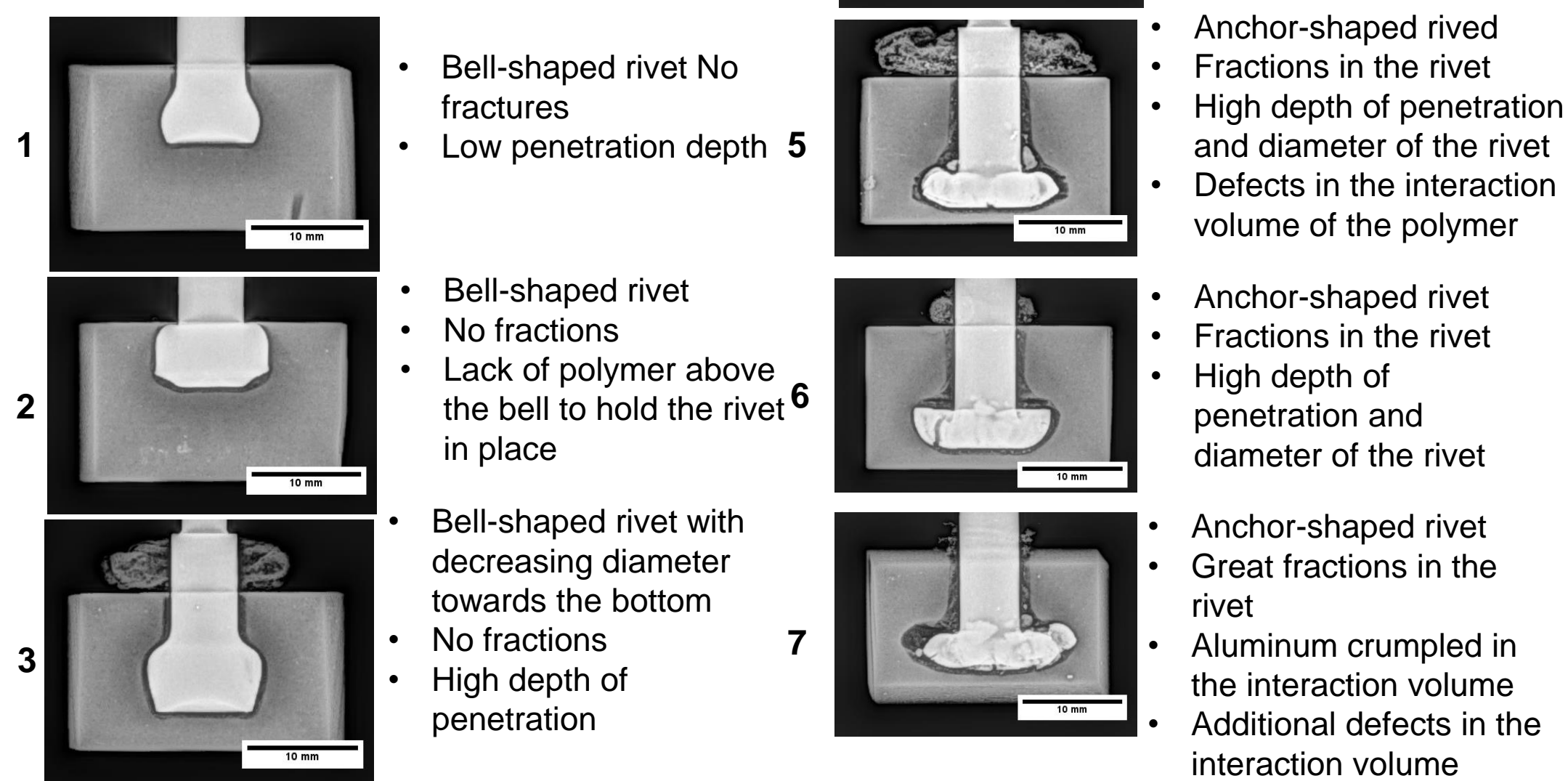


Figure 5: X-ray tomography of manufactured friction rivets

Pull-out test results

Pull-out test results are shown in the Fig 7, which does not include samples 3, 4, and 6, since those samples failed in the base material of the rivet. Three different failure modes observed (Figure 6):

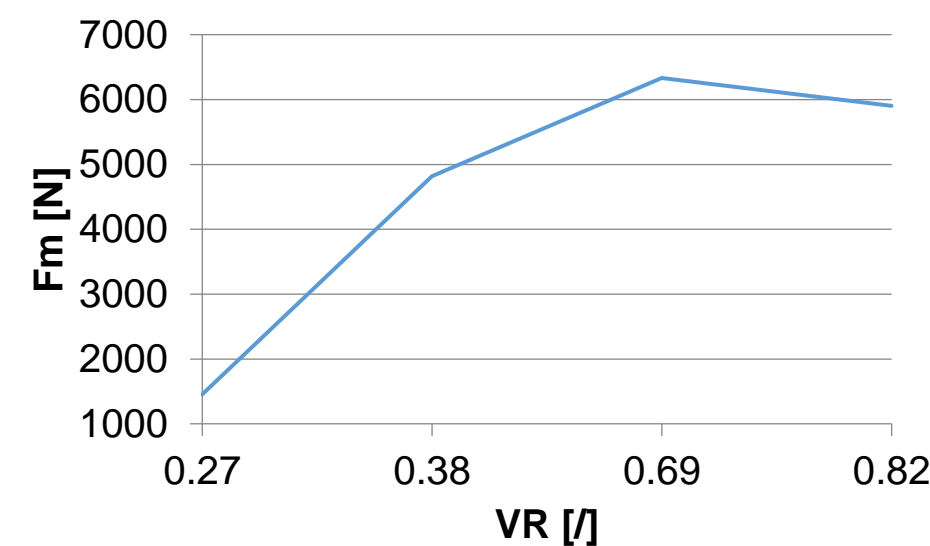
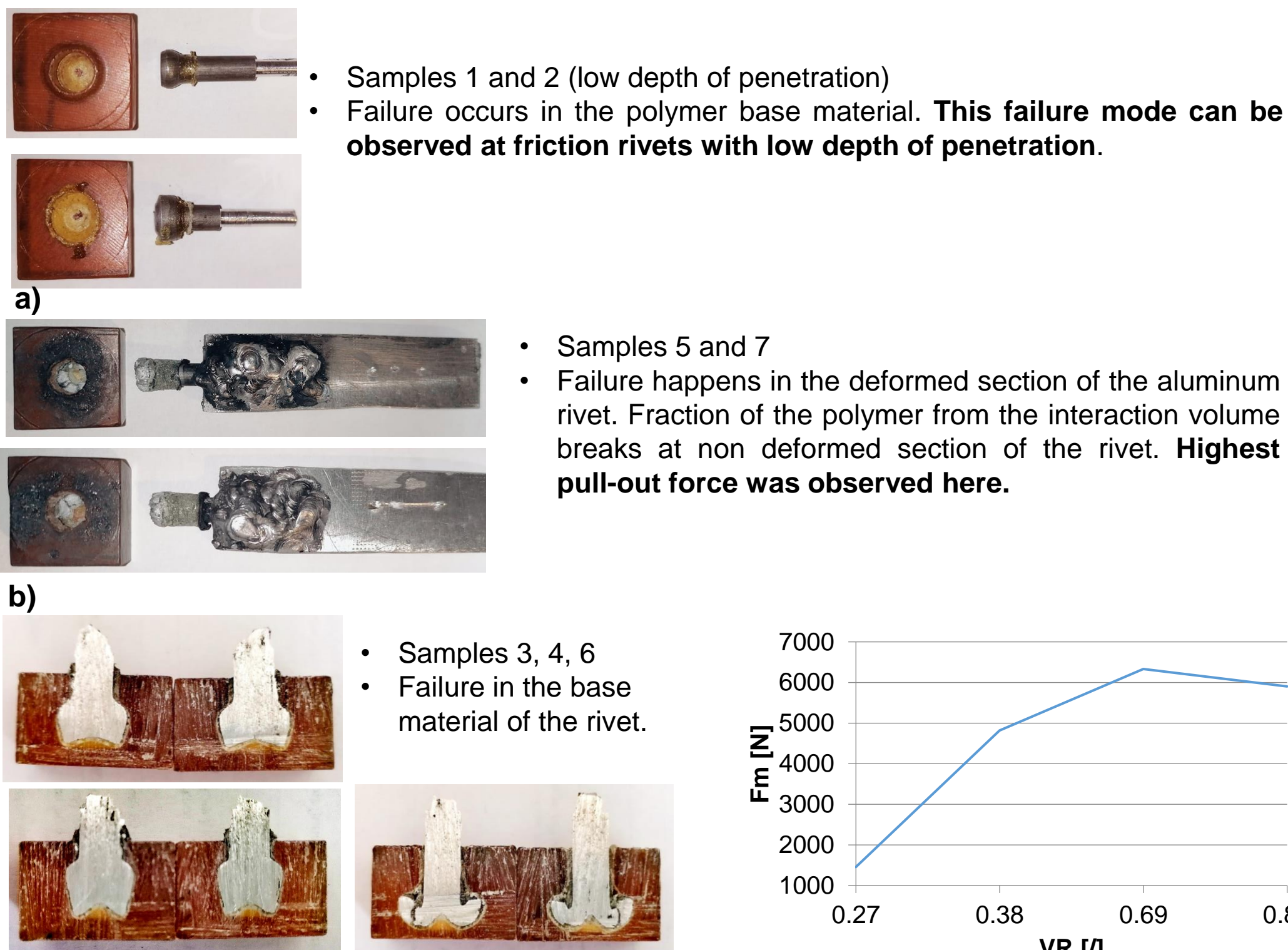


Figure 7: Pull-out force in relation to the volumetric ratio.

CONCLUSIONS

1. Recognized joint shapes:
 - Bell shape with decreasing diameter.
 - Bell shape with highest diameter at the end of the rivet.
 - Anchor shape.
2. Pull-out force increases with increasing VR. With increasing VR over 0,69 the pullout force shows decreasing trend
3. Three different failure modes at pull-out test:
 - Failure in the polymer base material.
 - Failure in the deformed section of the aluminum rivet.
 - Failure in the undeformed section of the aluminum rivet.
4. Two additional possible defects were recognized:
 - Crumpling of the aluminum rivet inside the polymer base material.
 - Defects in the interaction volume.